Acta Mechanica manuscript No.
(will be inserted by the editor)

Incompressible and Locking-free Finite Elements from Rayleigh Mode Vectors

Quadratic Displacements in Four-node Plane Elements

Gautam Dasgupta
Columbia University
New York, NY, USA
E-mail: dasgupta@columbia.edu

Received: date / Accepted: date

Abstract Under pure bending, with an arbitrary patch of plane four-node finite elements, the exact analytical algebraic expressions of deformation, strain and stress fields are numerically captured by a computer algebra program for both compressible and incompressible continua. The Ritz test functions are generated as linear combination of Rayleigh displacement vectors. These coupled fields model pure bending of Euler-Bernoulli beam with appropriate linearly varying axial strains devoid of shear. Such Courant "*admissible*" functions allow an undeformed straight side to curve in flexure. Since these displacement vectors satisfy equilibrium they are necessarily functions of the Poisson's ratio. Applications in bio-, micro- and nano-mechanics motivated this formulation that blurs the frontier between the finite and the boundary element methods.

Exact integration yields the shear locking-free element stiffness matrix for a compressible convex or concave quadrilateral, or a triangular element with a side node. For an isochoric plane strain problem, the Rayleigh kinematic mode of dilatation is replaced by a constant pressure. The equivalent nodal loadings are calculated according to the Ritz variational statement. Subsequently, without assembling the global stiffness matrix, nodal compatibility and equilibrium equations are solved in terms of Rayleigh modal participation factors.

The exact integral of a generic quadratic polynomial, which describes energy density fields, is furnished as a closed form algebraic expression that can be incorporated in `Fortran` or `C`$^{++}$ finite element calculations without resorting to any numerical quadrature.

Keywords exact integration · flexure modes · isochoric mode · symbolic computation

Department of Civil Engineering and Engineering Mechanics
School of Engineering and Applied Sciences

1 Introduction

The historic success of computational fluid dynamics [6], in real-world applications, encouraged innovations of novel techniques that minimized a functional with spatially and temporally discretized test functions. In this paper attention is confined to designing a finite element [8] methodology for two-dimensional linear static analysis of isotropic continua undergoing flexural and plane strain isochoric deformations.

Utilizing the Ritz variational formulation [42], in order to generate approximate solutions for boundary value problems of continuum mechanics, Courant proposed spatial discretization via triangulation [10] that was associated with linear displacement fields. Thus, for *all* problems of mathematical physics, because the partial differential equations are of second or higher order, homogeneous balance equations (*i.e.*, local or point-wise *strong* equilibrium conditions) are always satisfied. When the Ritz functional is accurately evaluated exact solutions for constant boundary stresses can be numerically reproduced by any collection (or *patch*) of elements of arbitrary geometrical shapes. This is the demand from Iron's *patch test.* [22,23]. The Courant triangulation yields constant stress fields, hence any such *patch* become 'too stiff' when the benchmark test of an Euler-Bernoulli beam is conducted. Therein, the constraint due to triangular shapes, under pure bending, contaminates all elements with shear stresses (because a patch of triangular elements cannot approximate a stress gradient without shear). This inaccuracy is known as *shear-locking*. Departures from basic exact solutions are associated with modeling deficiencies, and this class of phenomena, in general, is termed to be *locking* [30].

In order to improve the accuracy of Courant's triangular elements, Taig [46,47] introduced quadrilateral elements and the accompanying *isoparametric* formulation. The associated energy density functions (in the Ritz variational statement) were integrated numerically [21]. Based on Projective Geometry [43], Wachspress coordinates [48,19] (generalized barycentric coordinates [16]) allowed polygonal elements that resemble boundary elements[3,29]. Instead of *isoparametric* mapping, rational polynomials in the physical $x, y-$ frame formed the basis functions. The formulation was amenable to analytical evaluation of the energy integral ($\int \mathcal{B}^T \ \mathcal{D} \ \mathcal{B} \ d\Omega$ within each element Ω), [12]. Locking problems still persisted.

The reason is that neither Taig's isoparametric nor the Wachspress Padé formulation permits an edge of a quadrilateral element to curve. This is a kinematic requirement of the Euler-Bernoulli beam where only 'a plane section normal to the neutral axis remains plane' (and does not curve). Thus by constraining an element edge to remain straight, when it should curve in flexure, locking was invariably introduced.

This paper solves locking problems for a four-node plane element that can be a convex or concave quadrilateral or a triangle with a side node where the displacement vectors are obtained from Rayleigh displacement modes of quadratic polynomials that satisfy equilibrium in the *strong sense*. The resulting Ritz test functions, which are linear combination of Rayleigh modes, are

Courant "*admissible*" [10] because each independently satisfy static equilibrium.

For a benchmark (concave) finite element, detailed algebraic expressions are presented in Appendix-II. The necessary exact integration expression is included in Appendix-I. The computer mathematics environment *Mathematica* is extensively employed in concept development and numerical calculations.

Each deformation field associated with Courant's triangulation introduces a change in 'volume' (*i.e.*, area in plane strain cases). Consequently, for the limiting incompressible case of the Poisson's ratio $\nu = \frac{1}{2}$, it has been a daunting task to recover the constant element pressure $\wp$. The Rayleigh displacement vectors, which contain 'without shear the constant transverse gradient of an axial strain' (*e.g.*, flexural strains) and the 'constant dilatational distribution' independently, paved the solution to alleviate the difficulties with incompressibility and shear-locking.

The proposed formulation is not hybrid as Fix defines in [15] nor non-conforming/incompatible that is elaborated with historical references in [20]. Also, the choice of physically "*admissible*" [10] Ritz test functions followed by analytical integration (not any numerical quadrature whatsoever) to construct the element stiffness matrix insulate the present formulation from "variational crimes" [45]. MacNiels's defect-free characterization [31] is an appropriate description of what is achieved here with Rayleigh modes and exact integration.

Rigorous analyses of the numerical development of this paper can be traced back to various publications of Irschik (with co-authors); *e.g.*, [38] on the role of the Poisson's ratio in finite element basis functions, formulating the problem in the *natural* x, y frame [18] rather than *computational* η, ξ coordinates [46, 21], for continuum mechanics with source terms in bio-morphometric analysis [24]. Solutions for 'coupled displacement vectors' in bio-, micro- and nano-thermo-mechanical applications motivated this finite element formulation.

2 Formulation

The entire formulation is carried out in the 'x, y' physical (*not* 'η, ξ' computational) frame with element vertices (x_i, y_i) for node i. Calculations for compressibility, $\nu \neq \frac{1}{2}$, and incompressibility, $\nu = \frac{1}{2}$, require two different strategies to utilize the Ritz formulation. Then within each two classes, the constant strain problems must be addressed before the shear-locking phenomenon is modeled; also, the rigid body modes must be incorporated first. For four-node plane elements, there are eight nodal displacement degrees-of-freedom, consequently, eight independent physical criteria are to be selected here.

The standard notation of elasticity is used here:

$$\text{axial strains along } x, y : \epsilon_{xx}, \epsilon_{yy} \tag{1}$$

$$\text{axial stresses along } x, y : \sigma_{xx}, \sigma_{yy} \tag{2}$$

$$\text{shear strain and stress: } \gamma_{xy}, \tau_{xy} \tag{3}$$

In this paper to address shear-locking and incompressibility, the Rayleigh modes are:

(a) rigid body modes
  (i) mode-1: rigid body motion in the $x-$ direction
  (ii) mode-2: rigid body motion in the $y-$ direction
  (iii) mode-3: rigid body rotation on the $x-y$ plane
(b) constant strain fields
  (a) constant deviatoric strains
    (i) mode-4: $\epsilon_{xx} = -\epsilon_{yy} = c_1, \gamma_{xy} = 0$; c_1 : an arbitrary constant
    (ii) mode-5: $\epsilon_{xx} = \epsilon_{yy} = 0, \gamma_{xy} = c_2$; c_2 : an arbitrary constant
(c) constant (non-zero) delation
  (i) mode-6: $\epsilon_{xx} = \epsilon_{yy} = c_3, \gamma_{xy} = 0$; c_3 : an arbitrary constant
(d) to emphasize locking-free fields flexural modes are expressed in terms of stresses
  (i) mode-7: $\frac{\partial}{\partial y}\sigma_{xx} = c_4, \sigma_{yy} = 0, \tau_{xy} = 0$; c_4 : an arbitrary constant
  (ii) mode-8: $\frac{\partial}{\partial x}\sigma_{yy} = c_5, \sigma_{xx} = 0, \tau_{xy} = 0$; c_5 : an arbitrary constant

In modes-7 and 8 the stress gradient tensors implies that along $\mathbf{n}$ normal to any arbitrary direction $\mathbf{t}$, *i.e.*, $\mathbf{t} \perp \mathbf{n}$, $\frac{\partial}{\partial \mathbf{n}}\sigma_{\mathbf{tt}}$ is a constant.

The test functions for the Ritz variational formulation [42] are linear combination of Rayleigh modes. Since the displacement vector associated with each Rayleigh mode complies with all balance laws, all test functions for the Ritz variational formulation Courant "*admissible*" [10].

2.1 Three-node plane compressible elements

The incompressible cases are verified first to pass the uniform stress *patch tests*. In the $x-y$ frame the six Rayleigh vectors: $\psi_i = \begin{Bmatrix} u : x-\text{displacement} \\ v : y-\text{displacement} \end{Bmatrix}$ are:

(a) rigid body modes
  (i) mode-1: $\psi_1(x,y) = \psi_1 = \begin{Bmatrix} 1 \\ 0 \end{Bmatrix}$: rigid body motion in the $x-$ direction
  (ii) mode-2: $\psi_1(x,y) = \psi_2 = \begin{Bmatrix} 0 \\ 1 \end{Bmatrix}$: rigid body motion in the $y-$ direction
  (iii) mode-3: $\psi_3(x,y) = \begin{Bmatrix} -y \\ x \end{Bmatrix}$: rigid body rotation on the $x-y$ plane
(b) constant strain fields
  (a) constant deviatoric strains
    (i) mode-4: $\psi_4(x,y) = \begin{Bmatrix} x \\ -y \end{Bmatrix}$
    (ii) mode-5: $\psi_5(x,y) = \begin{Bmatrix} y \\ x \end{Bmatrix}$
(c) constant (non-zero) delation
  (i) mode-6: $\psi_6(x,y) = \begin{Bmatrix} x \\ y \end{Bmatrix}$

It is important to note that modes-1 through 5 yield zero dilatation as evidenced by:

$$< \frac{\partial}{\partial} x, \frac{\partial}{\partial} y > \odot \psi_I, I = 1 \ldots 5 \tag{4}$$

the subscript I signifies an incompressible mode.

a row vector is encased within angle braces $< >$ and

the dot product is indicated by $\odot$ (5)

The continuum displacements and nodal ones are connected via the Ritz (vector valued) test functions $\{\phi_i\}$:

$$\begin{Bmatrix} u \\ v \end{Bmatrix} = \sum_i^6 \{\phi_i(x,y)\}\, r_i;\ \phi_i(x,y) = \sum_j^6 \alpha_{ij}\ \psi_j(x,y);\ \phi_i : 2 \times 1 \text{ columns} \tag{6}$$

$\{r\}:$ displacements at degrees-of-freedom; α_{ij} : modal participation factors

i.e., α_{ij} indicates the contribution of mode-j to i-th. degree-of-freedom

Since for the $i\ th.$ node (x_i, y_i), the zero or unit displacement is dictated by the $i\ th.$ degree-of-freedom being zero or one, it can be shown that:

$$[\alpha]^T = \begin{bmatrix} \Psi(x_1,y_1) \\ \Psi(x_2,y_2) \\ \Psi(x_3,y_3) \end{bmatrix}^{-1} ; \Psi(x,y) = \{\psi_1, \ldots \psi_6\} : \text{size: } 2 \times 6 \tag{7}$$

Now the standard constitutive and strain displacement matrices $\mathcal{B}$ and $\mathcal{D}$ are used as the Ritz functional is minimized with respect to $\{r\}$ leading to the stiffness matrix:

$$[k] = \int \mathcal{B}^T\ \mathcal{D}\ \mathcal{B}\ d\Omega;\ \{R\} = [k]\,\{r\}\,; \quad \{R\}:\ \text{nodal force vector} \tag{8}$$

Since all elements of the strain energy density matrix ($\mathcal{B}^T\ \mathcal{D}\ \mathcal{B}$) are constants, one point quadrature leads to the exact integrals. Successful *patch tests* for uniform stresses verified the computer program. The detail numerical results are omitted here in the interest of brevity.

2.2 Three-node plane incompressible elements

Here a constant pressure $\wp$ replaces the dilatation mode-6, then:

$$\begin{Bmatrix} u \\ v \end{Bmatrix} = \sum_i^5 \{\phi_i(x,y)\}\, r_i; \quad \phi_i(x,y) = \sum_I^5 \alpha_{iI}\ \psi_I(x,y); \tag{9}$$

From the Ritz variational form the nodal loads R_i are expressed in terms of $\wp$ and α_{iI}. Equations of nodal equilibrium and compatibility are explicitly written out and the system of equations are solved for $\wp$ and α_{iI}. All symbolic calculations are carried out using *Mathematica*. The computer algebra programming is somewhat involved so only the results are presented here. The example in **Fig.** 1 captured the exact solutions for the following problem.

$$\textit{plane strain problem}; \quad \mu = \frac{1}{3}; \quad \nu = \frac{1}{2}; \tag{10}$$

nodes:{{0, 0}, {10, 0}, {10, 2}, {0, 2}, {0, 1}, {2, 2}}

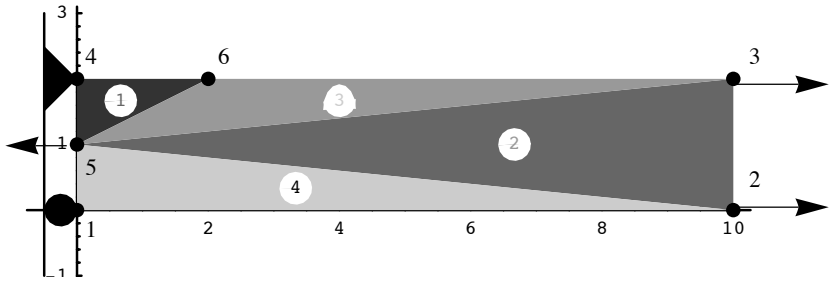

Fig. 1 Patch test with incompressible triangles: analytical fields are captured

Uniform unit stress blocks are replaced by horizontal forces at nodes, 2 and 3 by +1 and at 5 by -1, in the horizontal direction along the $x-$axis. For all elements identical pressures, stresses and strains were obtained from symbolic computation where exact results were captured:

$$\wp = \frac{1}{2}; \quad \{\sigma_x, \sigma_y, \tau_{xy}\} = \{1, 0, 0\}; \quad \{\epsilon_x, \epsilon_y, \gamma_{xy}\} = \left\{\frac{3}{4}, -\frac{3}{4}, 0\right\} \tag{11}$$

3 Four-node plane elements to accommodate pure bending

In the classical Courant triangulation, the *linear* fields $\psi_i(x, y), i = 1 \dots 6$, will satisfy any partial differential equation of mathematical physics. Beyond triangulations, the *coupled* interpolant Rayleigh modes are quadratic (or higher order) polynomials. The term *coupled* signify that one component of ψ_i depends on the other. Thus, the proposed method can be termed to be a Rayleigh *modal* formulation, as opposed to the conventional Courant nodal one when the *uncoupled* Ritz test functions: $\varphi_i = \begin{Bmatrix} S_k \\ 0 \end{Bmatrix}$ or $\begin{Bmatrix} 0 \\ S_\ell \end{Bmatrix}$, where $i = 1 \dots 8$; $k, \ell = 1 \dots 4$, are constructed directly from the Wachspress basis functions (generalized barycentric coordinates [16] including concavity and side node) $S_k(x, y)$, of the four-node plane element with vertices $(x_k, y_k), k = 1 \dots 4$, when the continuum displacement vector became:

$$\begin{Bmatrix} u \\ v \end{Bmatrix} = \begin{bmatrix} S_1, & 0, & S_2, & 0, & S_3, & 0, & S_4, & 0 \\ 0, & S_1, & 0, & S_2, & 0, & S_3 & 0, & S_4 \end{bmatrix} \{r\} = \{\varphi_i\}\{r\} = [\varphi]\{r\}; \tag{12}$$

where:$[\varphi]$ is (continuum) *field* (nodal) *displacement* transformation *matrix*.

Unlike equation (12) *i.e.*, equation (8) of [38], here, similar to equation (5) of [18] The Ritz test functions $\{\phi\}$, which are linear combinations of he Rayleigh flexural modes $\{\psi\}$, are functions of the Poisson's ratio ν. This makes

the proposed Ritz functions $\{\phi_i(\nu,x,y)\}$ a better choice than conventional shape functions $\{\varphi_i(x,y)\}$ in the light of Irschik and his co-authors' concern expressed in [38]:

> "The main problem of the standard continuum mechanics based formulation is the Poisson ratio ν which couples axial strains ... and the transverse normal strains ... in the stress strain relation ... ,"

The following choice alleviates the shortcomings in $\{\varphi\}$ via ψ_7, ψ_8 :

(a) plane strain

(i) mode-7: $\psi_7(\nu,x,y) = \left\{ \begin{array}{c} x\ y \\ \\ -\frac{1}{2}\left(x^2 + \left(\frac{\nu}{1-\nu}\right) y^2\right) \end{array} \right\}$

(ii) mode-8: $\psi_8(\nu,x,y) = \left\{ \begin{array}{c} -\frac{1}{2}\left(\left(\frac{\nu}{1-\nu}\right) x^2 + y^2\right) \\ \\ x\ y \end{array} \right\}$

(b) plane stress

(i) mode-7: $\psi_7(\nu,x,y) = \left\{ \begin{array}{c} x\ y \\ -\frac{1}{2}\left(x^2 + \nu\ y^2\right) \end{array} \right\}$

(ii) mode-8: $\psi_8(\nu,x,y) = \left\{ \begin{array}{c} -\frac{1}{2}\left(\nu\ x^2 + y^2\right) \\ x\ y \end{array} \right\}$

(c) plane strain incompressible

(i) mode-7: $\psi_7(\nu,x,y) = \left\{ \begin{array}{c} x\ y \\ \\ -\frac{1}{2}\left(x^2 + y^2\right) \end{array} \right\}$

(ii) mode-8: $\psi_8(\nu,x,y) = \left\{ \begin{array}{c} -\frac{1}{2}\left(x^2 + y^2\right) \\ x\ y \end{array} \right\}$

3.1 Compressible four-node elements

The computer algebra program, which has been tested with triangular elements in §2.1, now incorporates:

1. the flexural modes-7 and 8
2. exact integration, *vide*, Appendix-II, of quadratic polynomials to evaluate the element stiffness matrix from equation (8).

Dimensions of vectors (lists in computer algebra) and matrices (lists of lists) are evaluated as the calculation proceeds with the same code of §2.1.

3.1.1 General form for compressible media

In $\Re^n$ in an element with m nodes, there are $n \times m$ number of degrees-of-freedom. One needs, $n \times m$ number of Rayleigh vectors that can assure zero-locking for all physical phenomena like strain gradients as encountered in micro-mechanics.

In the interest of generalization the x, y and u, v nomenclature are replaced respectively by x_1, x_2 and u_1, u_2 in equation (6) leading to:

$$\text{for triangles: } \begin{Bmatrix} u_1 \\ u_2 \end{Bmatrix} = \left[\phi_i\right] \ \{r\} = [\Phi] \ \{r\}\,; \phi_i(x,y) = \sum_j^6 \alpha_{ij} \ \psi_j(x,y); \quad (13)$$

and with the inclusion of the flexural modes:

$$\phi_i(x,y) = \sum_j^8 \alpha_{ij} \ \psi_j(x,y); \ [\alpha] : 8 \times 8 \text{ matrix and } [\mathbf{\Phi}] : \ 8 \times 2 \qquad (14)$$

For a canonical concave element $[\mathbf{\Phi}]$ is in Appendix-II, equation (20).

Since Rayleigh mode vectors for elements beyond the Courant triangle couple the displacement components through the Poisson's ratio ν in the following equations all ψ are indicated with the argument ν.

Extension for an m-node element in $\Re^n$, with $nm = n \times m$, the analog of equation (6) follows, therein each nm Rayleigh mode ψ_i is a $n \times 1$ vector :

$$\begin{Bmatrix} u_1 \\ u_2 \\ \vdots \\ u_n \end{Bmatrix} = \sum_{i=1}^{nm} \{\phi_i\}\, r_i = [\Phi]\,\{r\}\,; \quad \begin{cases} \textit{summary of notations}: \\ \{\psi_i\} \quad : \text{ Rayleigh modes: } n \times nm \\ \{\phi_i\} \quad : \text{ Ritz test functions: } n \times nm \\ \{\varphi_i\} : \begin{cases} \text{field-displacement matrix: } n \times nm \\ \text{with } m \textit{ independent} \text{ basis functions} \end{cases} \end{cases}$$

matrix $[\ldots]$: a '*list of lists*' $\{\{\ldots\}, \{\ldots\}, \ldots\}$; (15)

$$\text{in general: } \phi_i(\nu, x_1, x_2, \ldots, x_n) = \sum_j^{nm} \alpha_{ij} \ \psi_j(\nu, x_1, x_2, \ldots, x_n); \qquad (16)$$

The modal participation factors are calculated as in equation (7). The nodal point coordinates of node-j is indicated with a superscript:

$$\text{for the first node the coordinates are: } \left(x_1^{(1)}, x_2^{(1)}, \ldots, x_n^{(1)}\right)$$
$$\text{for the } j-\text{th. node the coordinates are: } \left(x_1^{(j)}, x_2^{(j)}, \ldots, x_n^{(j)}\right), j = 1, m \quad (17)$$

$$[\alpha]^T = \begin{bmatrix} \Psi\left(\nu, x_1^{(1)}, x_2^{(1)}, \ldots, x_n^{(1)}\right) \\ \Psi\left(\nu, x_1^{(2)}, x_2^{(2)}, \ldots, x_n^{(2)}\right) \\ \vdots \\ \Psi\left(\nu, x_1^{(m)}, x_2^{(m)}, \ldots, x_n^{(m)}\right) \end{bmatrix}^{-1} ; \begin{cases} \Psi(x,y) = \{\psi_1, \ldots \psi_{nm}\} \\ \psi_i : \text{a vector of } n \text{ rows} \end{cases} \qquad (18)$$

The *Mathematica* program for the triangular element can be easily extended since all list operations (and matrix operations, when a matrix is structured as a list of lists) remain the same for equations (**??**) through (15) as equations (6) and (7).

The stiffness matrix expression equation (8) results from the Ritz variational formulation hence it is independent of m, n. However, the exact integration in the element bounded by hyper-planes in $\Re^{n-1}$ require (n-2) applications of the divergence theorem to convert the integral on a (plane) polygon.

3.1.2 Numerical Results: Locking-free exact response

Highlights from a series of numerical experimentations are presented now. Each node is numbered and each element number is shown within a white disc. The results are from a *Mathematica* program. The problem description is:

$$\text{Young's Modulus} = 1; \quad \text{Poisson's Ratio} = \frac{1}{4}; \quad \textit{plane stress problem;} \tag{19}$$

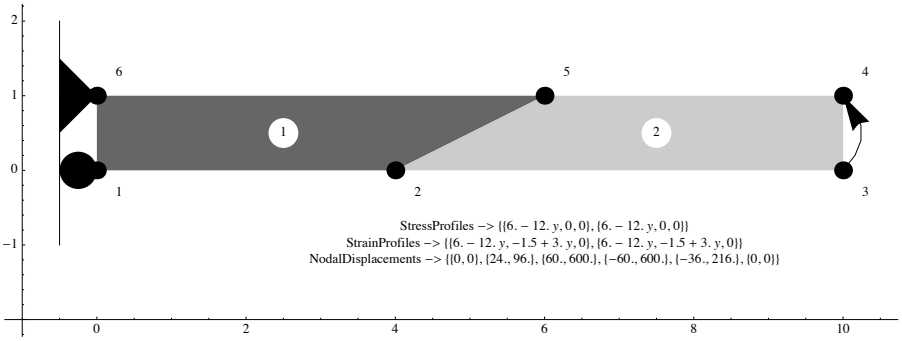

Fig. 2 Two element patch; horizontal forces: +1 at node 3, -1 at 4

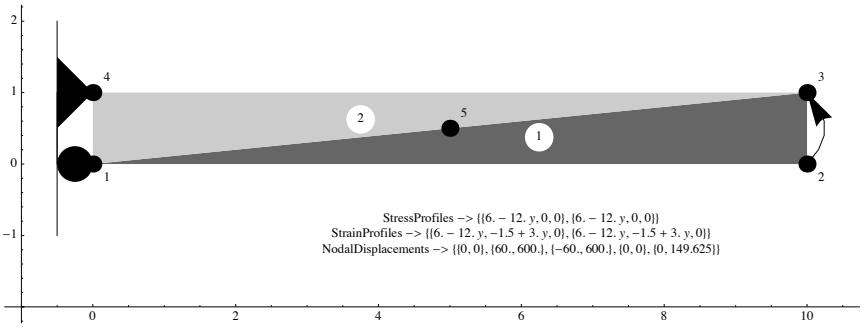

Fig. 3 Two triangles with side-nodes; horizontal force: +1 at node 2, -1 at 3

The stress, strain and displacement profiles are identical in both elements of **Fig.** 2 and **Fig.** 3. The calculations reproduced the analytical results. There is no shear stress (and strain) and the bending stresses (and strains) are linear in y:

$$\text{strains: } \{\epsilon_{xx}, \epsilon_{yy}, \gamma_{xy}\} = \{6 - 12y, 3y - 3/2, 0\} \tag{20}$$

$$\text{stresses: } \{\sigma_{xx}, \sigma_{yy}, \tau_{xy}\} = \{6 - 12y, 0, 0\} \tag{21}$$

The end $y-$displacement (vertical deflection) is 600 that matches the analytical result exactly.

3.2 Incompressible four-node elements

The modal participation statement, equation (9), is rewritten:

$$\begin{Bmatrix} u \\ v \end{Bmatrix} = \begin{bmatrix} \phi_i \end{bmatrix} \ \{r\} = [\Phi] \ \{r\} \, ; \phi_i(x, y) = \sum_{I \neq 6}^{8} \alpha_{iI} \ \psi_I(x, y); \tag{22}$$

and the *Mathematica* program of §2.2 is implemented. The exact results were obtained for the example in **Fig.** 4.

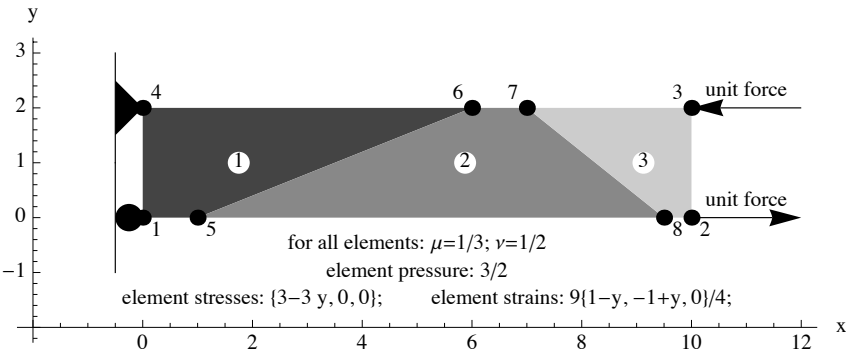

Fig. 4 A *Locking-free* test with incompressible elements

As it has been mentioned in §2.2, the intricate programming details are not included in this paper. Consequently, intermediate numerics are not presented.

3.3 Morphometric applications

A number of practical applications with the Wachspress formulation of 1971 [48] were reported in 1991 in [32] followed by [34,33]. The notion of concavity was detected in a later publication [13]. However, it was Irschik's formulation of 2003 with source terms in growth analysis [24,27] demanded high accuracies in shape-analysis with proper treatment of incompressibility and locking issues. This paper intends to furnish an accurate method for bio-medical applications.

4 Comments on Symbolic Computations

`Fortran` language,[1], was designed according to the imperative programming paradigm to carry out numeric calculations. Very soon after that, McCarthy released `LISP`, [36] as a functional programming language based on the $\lambda-$calculus, [7].

Contemporary revolution in digital computing made it possible to undertake very complicated, [50], symbolic and numerical computation in tandem. *Mathematica* meets the expectation of McCarthy's "common sense," [35], in computing. Immense theoretical progress, [5], can aid uniqueness proofs for the stress fields in equilibrium to be the best choice of Courant "*admissible*" set of Ritz *test functions*. Text books on finite elements, *e.g.*, [2], and general continuum mechanics, *e.g.*, [9], and especially, excellent material by Carlos A. Felippa, with detailed *Mathematica* codes to developing symbolic programs:
`http://www.scribd.com/doc/46188490/Reference-Fellipa`
is a very rich resource.

4.1 Experimentation with concave finite elements

Concave finite elements are extremely rare in the literature. Wachspress in 1975, [49], discussed the method to determine the the shape functions that are linear along the edges.

Recent interests on concave element have been motivated by biological growth analysis, [37]. Specifically in cranio-facial morphology, [13], concavity cannot be ignored. The invariant analysis of bio-morphometry, [41], demanded analytical formulations. Many of those legacy codes (of 1980) are still used, [4], in current research. Irschik's seminal work, reported in [27], laid out the framework for immediate applications in bio-morphology. His earlier work, in continuum mechanics related to source terms makes rigorous analytical formulations possible to model growth absorption and resorption that was initially introduced in 1982, [44], from an engineering perspective. Especially, the rational treatment, [26], makes it possible to characterize growth without landmarks, within the context of non-unique solutions, [25, 11].

The surface growth phenomenon, as opposed to the volumetric one, introduces concavities in biological objects. Thus Irschik's explicit representation, from 2003, of the mechanics of surface growth, [24], motivated the author to deploy the Wachspress formulation, [14] in 2008 to model compatible elements.

4.2 Scalar and vector field computations

The nondimensional parameter ν couples the displacement vectors via the equilibrium equation. *Mathematica* programs require very little modifications to handle scalar and vector objects side by side. From the physics of the problem the Buckingham Π-theorem, which is a formalization of the Rayleigh method for dimensional analysis, is thusadequately addressed in computation.

5 Conclusions

Closed form shear-locking free two-dimensional analytical results are reproduced devoid of "variational crimes [45]." Pian's *stress-based* formulation [40], where the Poisson's ratio dependent [38] Rayleigh flexure modes satisfied equilibrium, is carried out in a computer algebra environment (*Mathematica*) with *exact integration* (not any numerical quadrature). Thus, the Rayleigh modal displacement profiles are concluded to be the best Courant "*admissible*" candidates for the Ritz formulation.

Computer algebra has been indispensable during the concept development phase. Symbolic computation, which has been in the mind of pioneers [39], is anticipated to find wider applications in all research fields of engineering and sciences [50]. Now, with the advent of seamless translation into $\mathtt{C}^{++}$ codes, *e.g.*, [17], high accuracy finite element computations have become economical in engineering mechanics and computer graphics (to name a few) simulations especially with the *Graphics* or *Visual Processing Units* (GPU or VPU).

The computational steps developed here serve as building blocks in constructing other two- and three-dimensional defect-free elements [31]. For example, in eight-node three-dimensional elements, the 24 Rayleigh modes could be selected according to [28]. Integration on the element volume are to be converted to the boundary integrals by divergence theorem. Closed form results in the appendices can be utilized in procedural programs to carry out:

1. Qualitatively select the Rayleigh modes to be reproduced
2. For each mode, derive the analytical (coupled) displacement fields that satisfy equilibrium
3. Linearly combine the Rayleigh modes to obtain *shape vector* matrix: [**S**]
4. Solution of unknowns:
   (a) Compressible cases:
      i. Obtain $\mathcal{B}$ from [**S**]
      ii. Carry out *exact integration* in $\int \mathcal{B}^T \ \mathcal{D} \ \mathcal{B} \ d\Omega$
      iii. Solve for nodal displacements
   (b) Incompressible cases:
      i. Substitute all Raleigh modes pertaining to dilatation with $\wp$ and its spatial derivatives
      ii. Convert boundary traction, which consists of the applied ones and those obtained from $\wp$, to nodal loads
      iii. Write all equations of equilibrium and compatibility
      iv. Solve for nodal displacements and coefficients for $\wp$ and its spatial derivatives

Acknowledgements Columbia University, Science and Technology Ventures: `http://www.techventures.columbia.edu`,
supported the research leading to the U.S. Patent No. 6,101,450 (June 3, 1997) of Gautam Dasgupta for "Stress Analysis Using a Defect-Free Four Node Finite Element Technique." This paper is an enlarged version of unpublished formulations and results.

References

1. John Backus. Fortran programmer's reference manual. Technical report, IBM Corporation, New York, Oct. 15 1956. (Backus: project leader).
2. M. Asghar Bhatti. *Fundamental Finite Element Analysis and Applications: with Mathematica and Matlab Computations*. John Wiley, 2005. ISBN-13: 978-0471648086.
3. C. A. Brebbia and J. Dominguez. *Boundary Elements - An Introductory Course*. McGraw-Hill, 1992.
4. Bruno Buchberger. White-box blac-box strategies in symbolic computations. In *Wolfram Research Technical Report*, *Mathematica* Developers Conference, Rotterdam, The Netherlands, 1993. Wolfram Research, Chamaign, IL.
5. Bruno Buchberger. Overview on theorema. In Bruno Buchberger, editor, *Theorema Workshop*, Hagenberg, Austria, June 9, 10 1997. RISC-LinzInstitut für symbolisches Rechnen, Johannes Kepler Universität.
6. C.K. Chu. *Computational fluid dynamics*. AIAA Selecte reprint series. AIAA, 1973. AIAA Selected Reprint Series, Vol. 4, Computational Fluid Dynamics, C. K. Chu, Ed., 1968; Selected Papers in Physics, Vol. VI, The Physical Society of Japan, Tokyo, 1971.
7. A. Church. *The Calculi of Lambda-Conversion*. Princeton University Press, 1941.
8. R. W. Clough. The finite element method in plane stress analysis. In *Proceedings, 2nd Conference on Electronic Computation, A.S.C.E. Structural Division*, pages 345 – 378, Pittsburgh, PA, September 8 and 9, 1960.
9. Andrei Constantinescu and Alexander Korsunsky. *Elasticity with Mathematica: An Introduction to Continuum Mechanics and Linear Elasticity*. Cambridge University Press, New York, NY, USA, 1st edition, 2007.
10. R. Courant. Variational methods for the solution of problems of equilibrium and vibration. *Bulletin of the American Mathematical Society*, 49:1–29, 1943.
11. G. Dasgupta. Validity of Almansi theorems for anisotropic boundary elements. *Journal of Engineering Analysis*, 5(2):89–94, June 1988.
12. G. Dasgupta. Integration within polygonal finite elements. *Journal of Aerospace Engineering, ASCE*, 16(1):9–18, January 2003.
13. G. Dasgupta and J. Treil. Maxillo-facial frame: Finite element shapes. *The Mathematica Journal*, 8:235–246, 2001.
14. G. Dasgupta and E.L. Wachspress. Basis functions for concave polygons. *Computers and Mathematics with Applications*, 56(2):459–468, July 2008.
15. George M. Fix. Hybrid finite element methods. *SIAM Review*, 18(3), 1976.
16. Michael S Floater, Kai Hormann, and Géza Kós. A general construction of barycentric coordinates over convex polygons. *German Research*, 1(v):311–331, 2006.
17. Peter Fritzson, Vadim Engelson, and Krishnamurthy Sheshadri. *MathCode*: A system for C++ or Fortran code generation from *Mathematica*. *The Mathematica Journal*, 10(4), 2008.
18. Johannes Gerstmayr and Hans Irschik. On the correct representation of bending and axial deformation in the absolute nodal coordinate formulation with an elastic line approach. *Journal of Sound and Vibration*, 318(3):461 – 487, 2008.
19. J. L. Gout. Construction of a hermite rational interpoation Wachspress type finite element. *Computational Mathematical Applications*, pages 337–347, May 1979.
20. B. Hassani and S.M. Tavakkoli. Derivation of incompatible modes in nonconforming finite elements using hierarchical shape functions. *Asian Journal of Civil Engineering (Building and Housing)*, 6(3), 2005.
21. B. M. Irons. Quadrature rules for brick based finite elements. *International Journal of Numerical Methods in Engineering*, 3, April/June 1971.
22. B. M. Irons and A. Razzaque. *Experience with the patch test for convergence of finite elements method*. Academic Press, New York, 1972.
23. Bruce Irons and Sohrab Ahmad. *Techniques of Finite Elements*. John Wiley, 1980.
24. H. Irschik. On the necessity of surface growth terms for the consistency of jump relations at a singular surface. *Acta Mechanica*, 162, 2003.
25. H. Irschik. On eigenstrains without displacements. *Acta Mechanica*, 178, 2005.
26. H. Irschik. On rational treatments of the general laws of balance and jump, with emphasis on configurational formulations. *Acta Mechanica*, 194, 2007.

27. H. Irschik. A systematic treatment of growth terms appearing in continuum mechanics formulations for biological materials. In *Second International Conference on Algebraic Biology*, 2007. AB'07, RISC, Hagenberg, Austria.
28. M. J. Loikkanen and B. M. Irons. An 8-node brick finite element. *International Journal for Numerical Methods in Engineering*, 20(3):523–528, 1984.
29. M. E. MacAlarney. Use of the boundary element method for biological morphometrics. *Journal of Biomechanics*, 28(5), 1995.
30. R. H. MacNeal. *Finite Elements: Their Design and Performance*. Marcel Dekker, 1994.
31. Richard H. MacNeal. Toward a defect-free four-noded membrane element. *Finite Elements in Analysis and Design*, 5(1):31 – 37, 1989.
32. M. E. McAlarney, G. Dasgupta, M. L. Moss, and L. Moss-Salentijn. Boundary macroelements and finite elements in biological morphometrics: A preliminary comparison. presented at the computers in biomedicine conference. In K. D. Held, C. A. Brebbia, and R. D. Ciskowski, editors, *Computers in Biomedicine*, pages 61—72, Southampton, UK, 1991. Computational Mechanics Publisher.
33. M. E. McAlarney, G. Dasgupta, M. L. Moss, and L. Moss-Salentijn. Anatomical macro element in the study of cranial facial rat growth. *Journal of Cranial Facial Growth and Developmental Biology*, 12:3–12, 1992.
34. M. E. McAlarney, L. Moss-Salentijn, M. L. Moss, M. Basra, and G. Dasgupta. Macro/finite element meshes. In L.D. Lutes and J.M. Niedzwecki, editors, *Engineering Mechanics*, pages 960—963, College Station TX, 5 1992. Ninth Engineering Mechanics Conference,, American Society of Civil Engieers.
35. J. McCarthy. Programs with common sense. Technical report, National Physical Laboratory, Teddington, England, 1958. Paper presented at the Symposium on the Mechanization of Thought Processes.
36. John McCarthy. Recursive functions of symbolic expressions and their computation by machine, part i. Technical report, Massachusetts Institute of Technology, Cambridge, Mass., April 1960.
37. M. L. Moss. The functional matrix hypothesis revisited. *American Journal of Orthodontics and Dentofacial Orthopedics*, 112:8–10;221–226;338–341410–417, 1997.
38. Karin Nachbagauer, Astrid Pechstein, Hans Irschik, and Johannes Gerstmayr. A new locking-free formulation for planar, shear deformable, linear and quadratic beam finite elements based on the absolute nodal coordinate formulation. *Multibody System Dynamics*, 26:245 — 263, 2011. 10.1007/s11044-011-9249-8.
39. A. J. Perlis and K. Samelsøn. International algebraic language. Technical report, Comm. Assoc. Comp. Mach., 1958. Preliminary Report.
40. Theodore H. H. Pian and Chang-Chun Wu. *Hybrid and incompatible finite element methods*. CRC Press, 2006.
41. Andre Publico. *Tensorial Biomophometrics: Continuum, Discrete, Statistical Aspects*. PhD thesis, Columbia University, May 2000.
42. W. Ritz. Über eine neue methode zur lösung gewisser variationalprobleme der mathematischen physik. *Journal Reine Angew. Math.*, 135, 1908.
43. Pierre Samuel. *Projective Geometry*. Undergraduate Texts in Mathematics. Springer-Verlag, New York, NY, 1988.
44. R. Skalak, G. Dasgupta, M. L. Moss, E. Otten, P. Dullemeijr, and H. Vilmann. Analytical description of growth. *Journal of Theoretical Biology*, 94(1982):555 – 577, 1982.
45. G. Strang. *Variational crimes in the finite element method*, pages 689 — 710. Mathematical Foundations of the Finite Element Method with Application to Partial Differential Equations. Academic Press, New York, 1972. editor: A.K. Aziz.
46. I. C. Taig. Structural analysis by the matrix displacement method. Technical report, British Aircraft Corporation, Warton Aerodrome : English Electric Aviation Limited, 1961. SO 17: Internal Report.
47. I. C. Taig. *Structural analysis by the matrix displacement method*. Warton : English Electric Aviation Limited, 1962.
48. E. L. Wachspress. *A Rational Basis for Function Approximation*, volume 228 of *Lecture Notes in Mathematics*. Springer Verlag, 1971.
49. E. L. Wachspress. *A Rational Finite Element Basis*. Academic Press, 1975.
50. S. Wolfram. *A New Kind of Science*. Wolfram Media, NY, May 2002.

Appendix-I: Closed form expression for element stiffness evaluation

For four-node plane elements, the exact integrals of quadratic functions within non-rectangular regions can be computed using the closed form expression presented in this section. For a quadratic displacement fields in $x-y$ domain, the strain fields are linear in x and y and the energy density is a quadratic function in x, y. The following expression is applicable for convex and concave quadrilateral elements and triangles with one side node.

Let the element domain Ω be defined by:
$nodes = \{\{x1, y1\}, \{x2, y2\}, \{x3, y3\}, \{x4, y4\}\}$.
Then $\left(\int_{\Omega} (\mathrm{a1} + \mathrm{a2}\ x + \mathrm{a3}\ y + \mathrm{a4}\ x^2 + \mathrm{a5}\ x\ y + \mathrm{a6}\ y^2)\ d\Omega\right)$ is:

```
-(1/24) (y1 - y2) (2 a4 x1^3 + 2 a4 x1^2 x2 + 2 a4 x1 x2^2 +
        2 a4 x2^3 + 12 a1 (x1 + x2) +
        4 a2 (x1^2 + x1 x2 + x2^2) + 8 a3 x1 y1 +
        3 a5 x1^2 y1 + 4 a3 x2 y1 + 2 a5 x1 x2 y1 +
        a5 x2^2 y1 + 6 a6 x1 y1^2 + 2 a6 x2 y1^2 +
        (4 a3 (x1 + 2 x2) + a5 (x1^2 + 2 x1 x2 + 3 x2^2) +
        4 a6 (x1 + x2) y1) y2 + 2 a6 (x1 + 3 x2) y2^2) -
 (1/24) (y2 - y3) (2 a4 x2^3 + 2 a4 x2^2 x3 + 2 a4 x2 x3^2 +
        2 a4 x3^3 + 12 a1 (x2 + x3) +
        4 a2 (x2^2 + x2 x3 + x3^2) +
        8 a3 x2 y2 + 3 a5 x2^2 y2 + 4 a3 x3 y2 +
        2 a5 x2 x3 y2 +
        a5 x3^2 y2 + 6 a6 x2 y2^2 + 2 a6 x3 y2^2 +
        (4 a3 (x2 + 2 x3) + a5 (x2^2 + 2 x2 x3 + 3 x3^2) +
        4 a6 (x2 + x3) y2) y3 + 2 a6 (x2 + 3 x3) y3^2) +
 (1/24) (y1 - y4) (2 a4 x1^3 + 2 a4 x1^2 x4 + 2 a4 x1 x4^2 +
        2 a4 x4^3 + 12 a1 (x1 + x4) +
        4 a2 (x1^2 + x1 x4 + x4^2) + 8 a3 x1 y1 +
        3 a5 x1^2 y1 + 4 a3 x4 y1 + 2 a5 x1 x4 y1 +
        a5 x4^2 y1 + 6 a6 x1 y1^2 + 2 a6 x4 y1^2 +
        (4 a3 (x1 + 2 x4) + a5 (x1^2 + 2 x1 x4 + 3 x4^2) +
        4 a6 (x1 + x4) y1) y4 + 2 a6 (x1 + 3 x4) y4^2) -
 (1/24) (y3 - y4) (2 a4 x3^3 + 2 a4 x3^2 x4 + 2 a4 x3 x4^2 +
        2 a4 x4^3 + 12 a1 (x3 + x4) +
        4 a2 (x3^2 + x3 x4 + x4^2) + 8 a3 x3 y3 + 3 a5 x3^2 y3 +
        4 a3 x4 y3 + 2 a5 x3 x4 y3 + a5 x4^2 y3 + 6 a6 x3 y3^2 +
        2 a6 x4 y3^2 + (4 a3 (x3 + 2 x4) +
        a5 (x3^2 + 2 x3 x4 + 3 x4^2) + 4 a6 (x3 + x4) y3) y4 +
        2 a6 (x3 + 3 x4) y4^2)
```

with the following *sign correction*. If (twice the area) :
`(-(x2 - x4) (y1 - y3) + (x1 - x3) (y2 - y4))`
is negative then the sign of the above expression is to be changed.

Appendix-II:Exact algebraic and numeric Results

The element in **Fig.** 5 under plane strain was analyzed without round-off with: $nodes : \{\{-1,0\},\{0,0\},\{0,-1\},\{1,1\}\}; \nu = \frac{1}{5}$; Young's Modulus $= 1$

The mode shape matrix $[\mathbf{\Phi}]$, like equation (14) , was obained, where $[\mathbf{\Phi}]^T$:

$$\begin{bmatrix} -\frac{5}{18}\left(-x^2-4y^2\right)-\frac{16xy}{9}-\frac{13x}{18}+\frac{10y}{9}, -\frac{2}{9}\left(-4x^2-y^2\right)-\frac{20xy}{9}+\frac{8x}{9}+\frac{2y}{9} \\ -\frac{2}{9}\left(-x^2-4y^2\right)-\frac{20xy}{9}+\frac{2x}{9}+\frac{8y}{9}, -\frac{5}{18}\left(-4x^2-y^2\right)-\frac{16xy}{9}+\frac{x}{9}+\frac{5y}{18} \\ \frac{5}{6}\left(-x^2-4y^2\right)+\frac{16xy}{3}+\frac{x}{6}-\frac{7y}{3}+1, \frac{2}{3}\left(-4x^2-y^2\right)+\frac{20xy}{3}-\frac{8x}{3}-\frac{2y}{3} \\ \frac{2}{3}\left(-x^2-4y^2\right)+\frac{20xy}{3}-\frac{2x}{3}-\frac{8y}{3}, \frac{5}{6}\left(-4x^2-y^2\right)+\frac{16xy}{3}-\frac{7x}{3}+\frac{y}{6}+1 \\ -\frac{5}{18}\left(-x^2-4y^2\right)-\frac{16xy}{9}+\frac{5x}{18}+\frac{y}{9}, -\frac{2}{9}\left(-4x^2-y^2\right)-\frac{20xy}{9}+\frac{8x}{9}+\frac{2y}{9} \\ -\frac{2}{9}\left(-x^2-4y^2\right)-\frac{20xy}{9}+\frac{2x}{9}+\frac{8y}{9}, -\frac{5}{18}\left(-4x^2-y^2\right)-\frac{16xy}{9}+\frac{10x}{9}-\frac{13y}{18} \\ -\frac{5}{18}\left(-x^2-4y^2\right)-\frac{16xy}{9}+\frac{5x}{18}+\frac{10y}{9}, -\frac{2}{9}\left(-4x^2-y^2\right)-\frac{20xy}{9}+\frac{8x}{9}+\frac{2y}{9} \\ -\frac{2}{9}\left(-x^2-4y^2\right)-\frac{20xy}{9}+\frac{2x}{9}+\frac{8y}{9}, -\frac{5}{18}\left(-4x^2-y^2\right)-\frac{16xy}{9}+\frac{10x}{9}+\frac{5y}{18} \end{bmatrix} \tag{23}$$

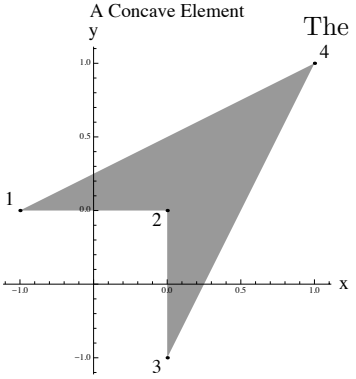

Fig. 5 A concave element

The $\mathcal{B}^T$: transposed strain-displacement matrix is:

$$\begin{bmatrix} \frac{5x}{9}-\frac{16y}{9}-\frac{13}{18}, -\frac{20x}{9}+\frac{4y}{9}+\frac{2}{9}, & 2 \\ \frac{4x}{9}-\frac{20y}{9}+\frac{2}{9}, -\frac{16x}{9}+\frac{5y}{9}+\frac{5}{18}, & 1 \\ -\frac{5x}{3}+\frac{16y}{3}+\frac{1}{6}, \frac{20x}{3}-\frac{4y}{3}-\frac{2}{3}, & -5 \\ -\frac{4x}{3}+\frac{20y}{3}-\frac{2}{3}, \frac{16x}{3}-\frac{5y}{3}+\frac{1}{6}, & -5 \\ \frac{5x}{9}-\frac{16y}{9}+\frac{5}{18}, -\frac{20x}{9}+\frac{4y}{9}+\frac{2}{9}, & 1 \\ \frac{4x}{9}-\frac{20y}{9}+\frac{2}{9}, -\frac{16x}{9}+\frac{5y}{9}-\frac{13}{18}, & 2 \\ \frac{5x}{9}-\frac{16y}{9}+\frac{5}{18}, -\frac{20x}{9}+\frac{4y}{9}+\frac{2}{9}, & 2 \\ \frac{4x}{9}-\frac{20y}{9}+\frac{2}{9}, -\frac{16x}{9}+\frac{5y}{9}+\frac{5}{18}, & 2 \end{bmatrix} \tag{24}$$

The lower triangle of the element stiffness matrix is:

$$\begin{bmatrix} \frac{5425}{1458} & & & & & & & \\ \frac{5575}{2916} & \frac{4325}{2916} & & & & & & \\ -\frac{2000}{243} & -\frac{2525}{486} & \frac{6725}{324} & & & & & \\ -\frac{7525}{972} & -\frac{5075}{972} & \frac{3275}{162} & \frac{6725}{324} & & & & \\ \frac{1340}{729} & \frac{1045}{729} & -\frac{5075}{972} & -\frac{2525}{486} & \frac{4325}{2916} & & & \\ \frac{8995}{2916} & \frac{1340}{729} & -\frac{7525}{972} & -\frac{2000}{243} & \frac{5575}{2916} & \frac{5425}{1458} & & \\ \frac{3895}{1458} & \frac{5395}{2916} & -\frac{1775}{243} & -\frac{7075}{972} & \frac{1385}{729} & \frac{8005}{2916} & \frac{3985}{1458} & \\ \frac{8005}{2916} & \frac{1385}{729} & -\frac{7075}{972} & -\frac{1775}{243} & \frac{5395}{2916} & \frac{3895}{1458} & \frac{7825}{2916} & \frac{3985}{1458} \end{bmatrix} \tag{25}$$